Modeling, Detection, and Disambiguation of Sensor Faults for Aerospace Applications

Edward Balaban, *Member IEEE,* Abhinav Saxena, *Member IEEE*, Prasun Bansal, Kai F. Goebel, and Simon Curran

***Abstract*—Sensor faults continue to be a major hurdle for systems health management to reach its full potential. At the same time, few recorded instances of sensor faults exist. It is equally difficult to seed particular sensor faults. Therefore, research is underway to better understand the different fault modes seen in sensors and to model the faults. The fault models can then be used in simulated sensor fault scenarios to ensure that algorithms can distinguish between sensor faults and system faults. The paper illustrates the work with data collected from an electro-mechanical actuator in an aerospace setting, equipped with temperature, vibration, current, and position sensors. The most common sensor faults, such as bias, drift, scaling, and drop-out were simulated and injected into the experimental data, with the goal of making these simulations as realistic as feasible. A neural network based classifier was then created and tested on both experimental data and the more challenging randomized data sequences. Additional studies were also conducted to determine sensitivity of detection and disambiguation efficacy to severity of fault conditions.**

***Index Terms*— modeling, transducers, fault diagnosis**

I. Introduction

SENSORS play a central role in modern systems to realize their full benefits of cost and performance. The degree of autonomy of these systems is highly correlated with the number of sensors used in those systems. Concepts like guaranteed uptime also mandate continuous state analysis with a respective increase in use of sensors.

However, as systems have become more reliable as a whole, sensors have attained the reputation as being the "weak link". Indeed, sensor failures have been responsible for highly publicized system breakdowns such as the aborted take-off of the space shuttle. Particularly for systems that require very high overall reliability combined with the need to keep weight low, there is a reluctance to add more sensors for that reason. Where sensors are used, they are configured with up to quadruple redundancy to be able to deal with sensor failure – which, as in the cited case, may not prevent operational disruption (depending also on the fault handling logic). This, in contrast to the general trend described above, has hamstrung the proliferation of system health management systems and consequently the potential technical advances of these systems.

Besides the weight addition, redundant sensors are not always feasible due to considerations of cost, space constraints, electrical/power constraints, and complexity increase. Any new sensor has to "work its way on-board".

It is therefore critical to have an understanding how sensors fail in order to mitigate the effects of off-nominal sensor behavior. While sensor fault detection and diagnosis are well addressed in the literature, there is no consensus on classification and nomenclature for sensor faults. Equally sparse are research efforts on characterization of the various classes of sensor faults and efforts to develop realistic sensor fault models that allow the simulation of fault effects and the study on the impact of the systems they are used in. Such models and associated simulations would also allow the study of sensor suit development; testing of fault detection, isolation, and recovery algorithms; and assessment of prognostic algorithm performance.

The paper starts with classifying and summarizing fault modes for the most common sensor types used in the aerospace industry. A brief overview of the state-of-the-art diagnostic techniques for sensor faults is then provided. After that the discussion shifts to describing experiments conducted by the team in simulating and diagnosing sensor faults. Finally, the results of the study are discussed and plans for future work outlined.

II. Sensor Fault Modes

Success of any health monitoring system heavily depends on the reliability of the employed sensors. In abstraction, a sensor fault may be defined as an unexpected deviation in the observed signal output in the absence of any anomalous condition in the system under test. Sensor faults occur due to various reasons, like manufacturing inefficiencies, wear and tear with long term usage, incorrect calibration, or

Manuscript received September 30, 2008. This work was supported by the NASA Aerospace Technology (AST) Integrated Vehicle Health Management (IVHM) program.

E. Balaban is with NASA Ames Research Center, Moffett Field, CA 94035 (phone: 650-604-5655, email: edward.balaban@nasa.gov)

A. Saxena is with Research Institute for Advanced Computer Science, NASA Ames Research Center, Moffett Field, CA 94035 (email: abhinav.saxena@nasa.gov)

P. Bansal is with Mission Critical Technologies, Inc, NASA Ames Research Center, Moffett Field, CA 94035 (email: pbansal@mail.arc.nasa.gov)

K.F. Goebel is with NASA Ames Research Center, Moffett Field, CA 94035 (email: kai.goebel@nasa.gov)

S. Curran is with Moog Inc., East Aurora, NY 14052 (email: scurran@moog.com)

mishandling. That often results in some physical deviation from design specifications within the sensor body, which in turn leads to unexpected outputs. From a fault tolerant control systems point of view, it is usually sufficient to identify the erroneous behavior of a sensor such that no unintended feedback is sent to the controller. System health monitoring is more concerned with the type of deviation observed from the normal expected output, irrespective of the actual physical damage that causes it. However, given the central role that sensor faults play in advancing system health management, it is imperative to have a good understanding of the various failure mechanisms within the sensors. Mapping failure mechanisms to resulting behaviors is critical to properly model sensor faults.

One can establish five basic behavioral sensor fault categories:

Bias: A constant offset from the nominal statistics of the sensor signal. Another way to describe bias is as the sensor output at zero input. Bias can occur due to incorrect calibration or physical changes in the sensor system. The governing equation is $Y_f = X + \beta + noise$, where β is the constant offset value. A time variant β results into drift failures.

Drift: A time varying offset from the nominal statistics of the sensor signal. Generally, only linear drifts have been modeled in the literature. However, a non-linear drift may be possible. Drift failures may be represented as $Y_f = X + \delta(t) + noise$, where $\delta(t)$ is the time varying offset factor.

Scaling (or *gain failure*): Magnitudes are scaled by a factor $\alpha(t)$ where the form of the waveform itself does not change [1]. Scaling can be represented by $Y_f = \alpha(t)^* X + noise$, where $0 < \alpha(t) < \infty$ is a scaling constant that may be time varying.

Noise: A random time series is observed. For analytical simplicity it is usually assumed that the noise is zero mean unless some information is available otherwise. It may be represented as $Y_f = noise$.

Hard Fault: The sensor output is stuck at a particular level expressed by $Y_f = C + noise$, where C is a constant. In general there are three sub-categories for hard failures.

1) Loss of Signal: represents the complete loss of sensor data where the output from the sensor is zero (C=0) [1].
2) Stuck Sensor: represents the situation where sensor output is stuck at a constant value.

Intermittents: Deviations from normal readings appear and disappear several times from the sensor signal. The frequency of such signatures is generally random. Intermittents can appear in any of the failure modes described above. Due to their random nature, they are the most difficult to track, identify, and account for in diagnostics algorithms.

Other categorizations exist - for example one that rates the quality of the sensor faults [2]. In particular, tame faults, are fault signals that are both close to nominal signal range and somehow correlated to it [1]. Faults such as bias and drift may fall into this category. Additive faults (like bias and drift) have been also classified into deterministic (constant offset) or semi-deterministic (offsets jump at random intervals and with random amplitudes) [3].

III. Sensed Phenomena

To be able to better model sensor faults, it is important to have an insight into the basic operating principles of the common sensors and the most common fault mechanisms. The phenomena discussed here include only those of most interest to aerospace systems, i.e. the ones encountered in temperature, acceleration, pressure, strain, force, load, current, and position measurements. Several other types of sensors commonly used in aerospace applications, such as attitude, direction, radiation, flow, and others, are left for future studies.

Measurements done by a sensor rely on a particular physical property or behavior of materials. With suitable infrastructure, these properties can be used to sense / measure several distinct phenomena. For instance, a resistance strain gage can be used to measure strain, stress, loads or pressure, depending on the application. The mechanism of a particular type of fault and its frequency depends, of course, on the physical design of the sensor. The sensor mechanisms covered and their corresponding uses (in italics) are as follows:

1) Thermocouples : *temperature*
2) Resistance Temperature Detectors (RTD) : *temperature*
3) Piezoelectric: *acceleration, vibrations, pressure, strain, force*
4) Piezoresistive: *strain, force, pressure, acceleration*
5) Resistive strain: *strain, force, pressure*
6) Hall Effect: *current, linear displacement*
7) Magnetostrictive effects: *linear displacement*
8) LVDT: *linear displacement, acceleration*

This list is certainly not complete, but is representative of the more commonly used sensors. Lastly, it needs to be mentioned that while the root causes of a sensor fault can be either a failure of the sensing mechanism itself or of the electrical system interpreting the data, only the former cases are discussed in this paper.

A. Thermocouples

Thermoelectric EMF is created in the presence of a temperature difference between two different metals or semiconductors. Thermocouples use this effect, called the Seebeck effect [4], to detect the temperature difference between two sources. A thermocouple circuit consists of two metals, e.g. copper and constantan, with two junctions at temperature To (test junction) and Tr as reference temperature (Fig. 1). Thermocouples have the widest temperature range of all sensor technologies, -200 to +2315°C, and can be used in a wide variety of environments [5].

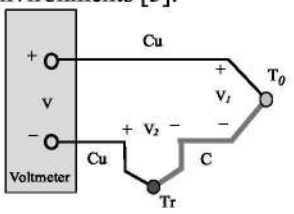

Fig. 1 : Thermocouple with External Reference Junction [6].

Faults in Thermocouples:

1) Degradation, corrosion or breakage of junction leading to bias, scaling, intermittent and/or complete failure [6].
2) Inhomogeneous changes in composition of the material taking place due to long exposures to high temperatures, resulting in thermoelectric drift.[7, 8].
3) When a thermocouple is bonded to a test surface, degradation of this bond may lead to the junction being at a lower temperature than the body, thus causing a bias.
4) A short (or degradation) in the lead wires due to temperature, leading to complete failure, bias, or drift [4].
5) Change in the reference temperature leading to bias [6].
6) Change in the thickness of the conducting leads causing a change in resistance, leading to a scaling error.

B. Resistance Temperature Detectors (RTD)

In an RTD, resistance increases with rise in temperature [4] due to the positive temperature coefficient of electrical resistance of metals. Precision RTDs consist of a thin insulated platinum wire encapsulated in a ceramic or metallic casing (Fig. 2). These casings are then immersed into the fluid or bonded to the surface for temperature measurement. Their normal operation range is –184.44°C to 648.88°C in this range they are both more accurate and have more linear characteristics than thermocouples [4]. No reference temperature is needed for the RTDs, but they have to be calibrated carefully at a particular temperature.

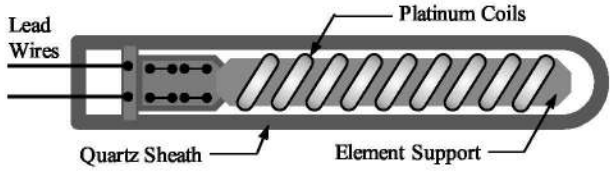

Fig. 2 : A standard Platinum Resistance Thermometer [5].

Faults in RTD's:

1) Over time exposure to high temperatures can cause a drift in the values of the RTD to several degrees per year [4].
2) A current passing through the RTD causes self heating of the element that can lead to a bias in the readings [4, 9].
3) Thin Film RTDs experience change in resistance due to surface stresses, which can lead to a bias in the readings.
4) Shock and vibration put strain on resistive wire and change its characteristics, leading to drift [4].
5) Degradation of insulation can cause a short between the coils and result in a lower resistance reading, leading to bias [4].

C. Piezoelectric sensors

Piezoelectricity is the ability of some materials (certain crystals and ceramics) to generate an electric potential in response to applied mechanical stress. A typical piezoelectric sensor consists of a piezoelectric crystal which is bonded to the surface of interest. Electrodes are connected to the either end of the crystal to sense the electric potential (charge) which can then be related to the stress experienced by the crystal - using piezoelectric and stress coupled equations (Fig. 3). They have a wide frequency range, from 0.01 Hz to 1 MHz [5], and temperature range from -270°C to +650°C.

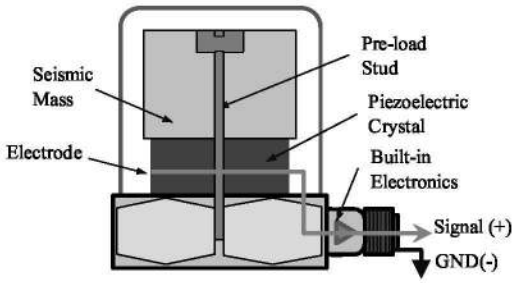

Fig. 3 : Piezoelectric accelerometer in compression mode [5].

Depending on the type of stress applied, a piezoelectric crystal can be used for sensing the following properties [4]:

1) Accelerations, from the stress induced in the piezoelectric crystal by a seismic mass (compression, flexure, or shear modes).
2) Vibrations, when mounted directly onto a surface.
3) Strain, when a thin piezoelectric crystal is bonded to a surface.
4) Pressure, either sensed directly by a piezoelectric disk (for high pressure applications) or via strains induced in a diaphragm.
5) Forces, by transmitting them directly through the crystal.

Faults in piezoelectric sensors:

1) Debonding due to degradation of the interface between the piezoelectric crystal and the substrate (or the seismic mass) over time can lead to either lower stresses being transferred between them resulting in a scaling error (scale factor < 1) or a change in the frequency response of the crystal, which may, in turn, affect high frequency behavior of the sensor [10].
2) Cracking of the crystal due to fatigue or shock causes scaling of the outputs from the sensor or a frequency shift of the sensor [11].
3) Depolarization of the crystal takes place if the crystal is subjected to temperatures above the operating range, even for a small time, that can result in a partial or complete loss of sensing capabilities [12].
4) Electric or mechanical fatigue of the crystal over time causes loss of polarization of the crystal, leading to scaling errors in the sensor [12].
5) Loss of contact between the crystal and the lead wires over time due to fatigue or shock can lead to intermittent or complete failure.
6) Temperature variations can lead to a change in the electro-mechanical properties of the crystals, resulting in bias or drift.

D. Piezoresistive sensors

The piezoresistive effect is the change in electrical resistance of a material due to applied mechanical stress (which is different from the change in resistance due to dimensional changes, as in a strain gage). Ceramics (or

semiconductors) are typically used as the sensing material since metals have very high gage factors (Fig. 4). Piezoresistive sensors can be used in static applications and moderately high frequencies up to 2500 Hz [4] and in thermal environments as high as 540°C [5]. Their operating range is up to 25G and they can withstand shocks of up to 2000G [9]. The principles of operation of piezoresistive sensors are the same as that of piezoelectric sensors, with the difference in the frequency range and shock characteristics. Piezoresistive sensors can be configured in the same ways as piezoelectric ones - to sense accelerations, forces, strains, pressures and low frequency vibrations.

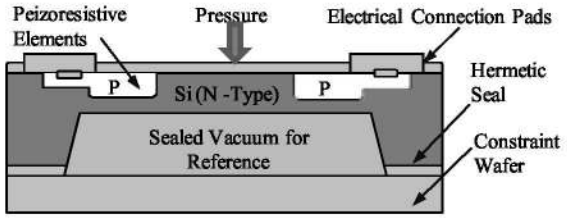

Fig. 4 : An absolute pressure sensor with a hermetically sealed vacuum reference chamber on one side of the sensing element [5].

Faults in Piezoresistive Sensors:

1) Debonding of the interface between the piezoresistive element and the substrate can lead to a lower degree of stresses transfer to the piezoresistive element, which in turn can lead to a scaling error.
2) Cracking of the piezoresistive element due to excessive fatigue or shock can lead to a scaling error and, in extreme cases, a complete failure.
3) Loss of contact between the element and the lead wires or electrodes can lead to intermittent or complete failure of the sensor.
4) Temperature variations can lead to a change in the electro-mechanical properties of the element, leading to bias in the readings.

E. Resistive Strain Gage

Resistive strain gages rely upon the change in the resistance due to the dimensional changes in the material (as opposed to change in material characteristics for piezoresistive materials) [9]. These gages consist of a grid of very fine wire or foil bonded to a backing (Fig. 5). The electrical resistance of the grid varies linearly with strain. Strain gages are good for detecting local strains, but have lower gage factors than the piezoresistive gages, which is compensated for by making them larger in size. They can generally be used only in applications which are static or have low vibration frequencies. Strain gages are also used in load cells or pressure transducers by measuring the stresses in the diaphragm, and in some cases, for measuring temperatures [5].

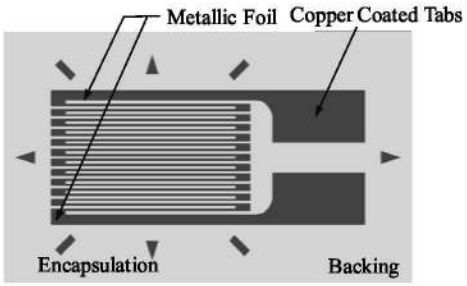

Fig. 5: A Typical Foil Strain gage [13].

Faults in Strain Gages:

1) Gaps in the bonding layer between the strain gage and the substrate lead to either bias or scaling error, depending on the nature of the void. Debonding of the gage will result in the same faults. This is of critical importance since the bond area in a strain gage is much larger than that in piezoresistive or piezoelectric sensors [6].
2) Fatigue of the wire or foil can lead to cracks, causing either bias or scaling (change of gage factor) fault. In extreme cases, complete failure may occur [13].
3) Temperature variations between the loaded and the temperature-compensated strain gage can lead to bias [13].
4) Loss of contact between the lead wires and the tabs on the strain gage leads to intermittent or complete failure of the sensor.

F. Hall effect sensors

A voltage potential V_H, called Hall voltage, appears across a conductor when a magnetic field is applied at right angles to the current flow. Its direction is perpendicular to both the magnetic field and the current and its magnitude is proportional to both the magnetic flux density and the current (see Fig. 6)

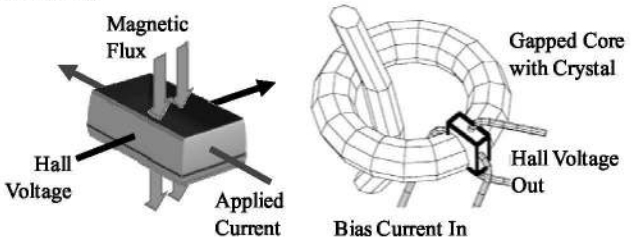

Fig. 6: a) Hall effect in a conductor, b) a hall effect current sensor [4].

The magnetic field causes a gradient of carrier concentration across the conductor A larger number of carriers on one side of the conductor, compared to the other side, causes a voltage potential V_H, [4]. Typically a ferrite crystal around a current carrying conductor is used to concentrate the magnetic field of the current, around a sensor. A bias current is then applied to the sensor and Hall voltage measured, which is proportional to the current in the main conductor. A Hall effect displacement sensor can utilizes a Hall sensor and a movable magnet, with an output proportional to the distance between the two.

Faults in Hall effect sensors:

1) Flaws in the core, such as degradation (corrosion, cracks), residual magnetic fields, or core breakage can result in a bias.
2) Changes in the bias current through the sensor can result in bias or scaling.
3) Temperature variations can change the magnetic properties of the ferrite core, resulting in decrease (or increase) of the induced magnetization, causing a bias in the readings.
4) Changes in the orientation of the induced magnetic field in the sensor (due to mechanical shocks or other reasons) can change the value of Hall voltage and lead to a scaling error.

G. Magnetostrictive Sensor

Ferromagnetic materials such as iron and nickel display the property of magnetostriction, where application of a magnetic field causes a strain in the crystal structure, resulting in a change in size and shape of the material [4]. To measure displacement, a moving magnet forms the "target", marking the position. The magnet's field, acting on a magnetostrictive wire, creates an ultrasonic pulse in the wire when a current pulse is passed through the wire. The time interval from the current pulse to the detection of the ultrasonic pulse at the end of the wire is used to determine the position of the magnet along the wire (Fig. 7) [9].

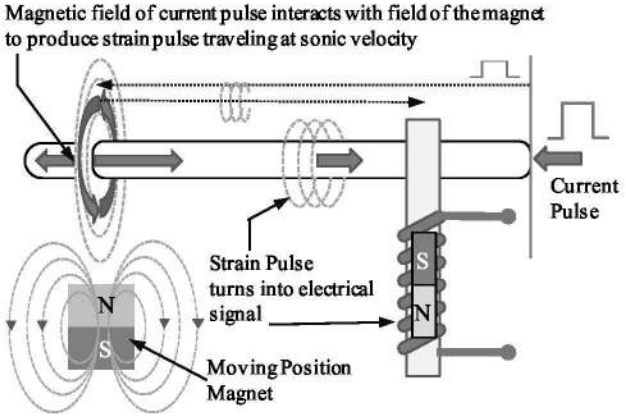

Fig. 7: Magnetostrictive principle for displacement measurement [14].

Faults in magnetostrictive sensors:

1) Changes in temperature cause a change in the velocity of propagation of sound through the magnetostrictive wire, which can lead to bias. Temperature also changes the magnetostrictive properties of materials, resulting in a bias [15].
2) Degradation (corrosion) of the ferromagnetic wire can lead to changes in the magnetosctrictive and ultrasonic properties, resulting in bias.
3) Loss of contact at the receiving end for the strain pulses can result in intermittent or complete failure.
4) Stray magnetic fields (particularly strong fields) can cause a random error in readings or result in excessive noise.

H. Linear Variable Differential Transformer (LVDT)

An LVDT is a position-to-electrical sensor whose output is proportional to the position of a movable magnetic core. The core moves linearly inside a transformer consisting of a center primary coil and two outer secondary coils wound on a cylindrical form (Fig. 8). The secondary windings are wound out of phase with each other. Moving the core, results in a differential voltage between secondary coils, which varies linearly with the core's position [5]. The LVDT can be coupled with a spring-mass system to detect the displacement of the spring to measure acceleration or force [4].

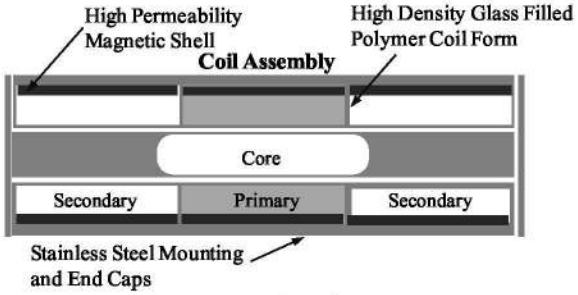

Fig. 8: Construction of a LVDT [4].

Faults in LVDT's:

1) Short in one of the coils can lead to either a bias or complete failure of the sensor.
2) Leakage of magnetic fields between the secondary coils can lead to a bias [5].
3) Changes in the primary voltage lead to a smaller induced voltage in the secondary, leading to a scaling error.

Table 1 shows the range and median for the different fault classes that have been found in the literature. This will provide an aid in modeling the sensor faults with realistic magnitudes when superimposed onto real data. It will also allow simulation of diverse sensor faults and subsequent training of algorithms to detect these sensor faults and distinguish them from system component faults. The number of references in literature showing actual sensor faults is found to be very limited; hence we list these statistics for a range of different sensors.

TABLE 1 : TYPICAL RANGES FOR SENSOR FAILURE VALUES AS AVAILABLE FROM THE LITERATURE.

Fault	Range	Median	Remarks	Sensors & References
Bias	1.2% to 60%	20%	% change over the nominal value	Unknown [16] Air flow [17] Temperature, Fuel Flow, rotor speed [18]
Scaling	0.3 to 0.7	0.45	Scale Factor	Piezoelectric [10, 12] Accelerometers [1]
	2.5 to 4.8	3.28	Scale Factor	Accelerometers [1]
Drift	6% to 75%	29%	% change over the nominal value, reported at the end of the drift (or data set)	Unknown [16] Fuel Flow [17] Temperature [18]

Noise	2.5% -to 250%	20%	% peak to peak values over the nominal value	Unknown [16] Pressure [17] Temperature, Fuel Flow, rotor speed [18] Accelerometers [19] Gyroscope [20]
Intermittent Dropout	2 to 10 drops	8 drops	Over a range of 20% to 29% of the reported data set, with median range of 23%	Unknown [16]

IV. Sensor Fault Detection and Identification (FDI) Techniques

The problem of fault detection and disambiguation has been approached from various angles in the past three decades. A wide variety of techniques have been reported; they can, however, be categorized into four basic categories. The emphasis on each of these categories has changed with time and all come with their own strengths and shortcomings. A brief overview of such approaches is presented here.

Most of the early work has focused on model-based sensor fault detection and disambiguation methods which, in general, require mathematical models of the system under investigation and utilize analytical redundancy generated by these models [3, 21]. The majority of these approaches first compare the observed sensor output and parameter estimates obtained from the model to compute residuals. There are few distinct categories for model-based approaches [22]. Parity approaches compute a residual vector that is zero when no fault is present and non-zero otherwise, to detect that a fault has occurred. Various parity approaches include Parity Space Approach (PSA) [23], Parity Equation Approach (PEA) [24], Generalized Likelihood Ratio Test (GLT), and Least Square Residual Approach (LSRA). Another approach is based on Bank of Observers (state estimators) that offer to cancel out the contribution of noise and model inaccuracies [25-27]. State Estimation Approaches based on Kalman Filters generate an estimate that can be used to compute residuals by comparing it with measured states [28, 29]. Other model based approaches include Fault Detection Filters [3], and Parameter Identification Approaches [30] that model various faults and track corresponding model parameters. Sometimes, the performance of analytic redundancy based FDI techniques is limited by modeling uncertainties.

In the recent years a great emphasis has been laid on data-driven methods as well, where signal processing and artificial intelligence techniques are employed. Such techniques are especially important in situations where the complexity of the system make it extremely difficult to model. These methods are relatively simpler and quicker to implement. Features are computed using standard statistical estimates or utilizing specialized domain knowledge [31, 32]. Various machine learning approaches, like Artificial Neural Networks (ANN), are very popular in the literature. Furthermore, expert system based approaches have also been used, where history data is used to construct a set of rules to diagnose system and sensor faults. Hybrid techniques have been developed to complement various individual techniques. For instance, in [24] authors propose a hybrid method that combines Parity Equation Approach (PEA) with wavelet based signal processing to avoid the need of a mathematical model of the aircraft. A pseudo model-based approach based on Principal Component Analysis (PCA) has been proposed in [29] where PCA is used to compute residuals in the absence of a mathematical model.

Therefore, a significant emphasis has been laid on generic fault detection techniques borrowing ideas from system diagnostics; however, the efforts on detecting specific sensor faults are less evident. In the absence of real sensor fault data it may be desirable to simulate realistic fault scenarios and develop specific techniques that will address more robust solutions to sensor fault detection and disambiguation from system faults. That will, in turn, improve the confidence on overall system diagnostics.

V. Experimental Setup

A ballscrew electromechanical actuator was used as the plant in our experiments. The experiments were performed on a test stand located at Moog Inc. The test actuator (Moog MaxForce 883-023) was connected to the hydraulic load cylinder by a rotating horn. Control and data acquisition were performed by real-time software running on dSPACE platform. Table 2 contains a list of all of the sensors used on the test platform, as well as their associated sampling frequencies.

Vibration was measured at four points on the test actuator, as shown in Fig. 9. All three axes of vibration were measured, with an additional measurement in the Z-direction by the accelerometer mounted directly on the nut of the ball screw. Temperature measurements were provided by a T-type thermocouple on the nut and an RTD embedded in the stator of the motor, as shown in. Fig. 9. Load is sensed by a Model 75 Sensotek 50,000 lbf. load cell. The position of the rod end of the test actuator was measured by a Trans-Tek 0219-0000 Linear Differential Voltage Transducer (LVDT).

TABLE 2 : List of sensors.

Measurement	Sensor	Type	Sample Rate
Load	Model 75 Sensotec Load Cell	Bonded foil strain gage compression and tension	3 kHz
Position	Trans-Tek 0219-0000	LVDT	3 kHz
Nut Temperature	T-type Thermocouple	Copper-constantan thermocouple	3 kHz
Motor Temperature	Integrated Stator RTD	RTD (thermistor)	3 kHz
Torque Producing Current	T200 Motor Drive Output	Hall effect sensor	3 kHz
Motor Velocity	T200 Motor Drive Output	Resolver	3 kHz
3-Phase Currents	(3) LEM LA 25-P Current Transducers	Closed loop (compensated), works on Hall effect	24 kHz
X-Y-Z Accelerometers	(3) PCB Model 352A24	Piezoelectric ceramic, shear	24 kHz

Nut Accelerometer	PCB Model 352A24	Piezoelectric ceramic, shear	24 kHz

LEM LA 25-P current transducers were used on each motor phase to sense the phase currents. For data acquisition, the Moog T200 motor drive output an analog signal representing the torque producing current, as well as the motor velocity.

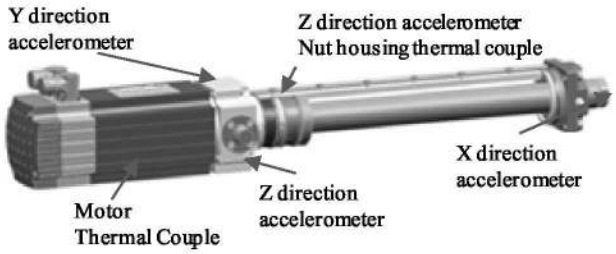

Fig. 9 : Location of sensors on Moog MaxForce 883-023 actuator.

A. Tests Performed

Table 3 describes the types of mechanical component fault cases introduced during the tests.

TABLE 3 : DIFFERENT EXPERIMENTS PERFORMED WITH SEEDED MECHANICAL COMPONENT FAULTS.

Experiment Set	Description
Baseline	Data collected with a nominal actuator just before the first set of ball return jam tests.
One Ball Return Jammed	One of the return channels fully blocked. Simulates obstruction of the return channel by a detached piece of insulation or other debris.
Repeatability	Tests to determine whether disassembly and reassembly of actuators affects test results. Five back to back runs were conducted.
Backlash	Tests with undersized balls to simulate backlash (freeplay)
Spalling	The purpose of this series of tests was to determine if a surface flaw (spall) can be detected using the actuator sensor suit. Three flaws have been electro-discharge machined into the screw of the actuator. The flaws were machined into the entire root of the screw forming a continuous flaw from crest to crest.

Sensor faults were injected a posteriori, as described in the next section. Permutations of the following conditions were used to run 2 x 2 x 2 = 8 scenarios for each of the mechanical component fault cases:

Motion profile: sinusoid or triangular wave

Load type: constant or spring

Load level: low (860 lbs spring force, 900 lbs constant force) or high (1725 lbs spring force, 1800 lbs constant force)

For the purposes of training and testing the neural network based classifier, described in the subsequent sections, extended duration scenarios were created using the collected data. These scenarios were designed to preserve the character of the collected data as much as possible, while extending the duration to 180 seconds. They contain two segments each – nominal, to represent a healthy system before the fault occurred and a faulty segment (90 seconds each). Since on the test stand the faults had to be seeded before the start of the tests, due to hardware limitations, nominal data was chosen from the experiments conducted under the same conditions. The total number of scenarios produced was 48 - 8 (conditions) x (2 components faults + 4 sensor faults).

VI. SENSOR FAULT SIMULATIONS

Bias: in our experiments bias, injected into temperature sensor data, was specified as percentage of the average baseline temperature (80F), calculated over the set of nominal (no fault injected) scenarios. Gaussian noise was then introduced into the actual amount of bias added, with a signal-to-noise ratio of 5 (see Fig. 10).

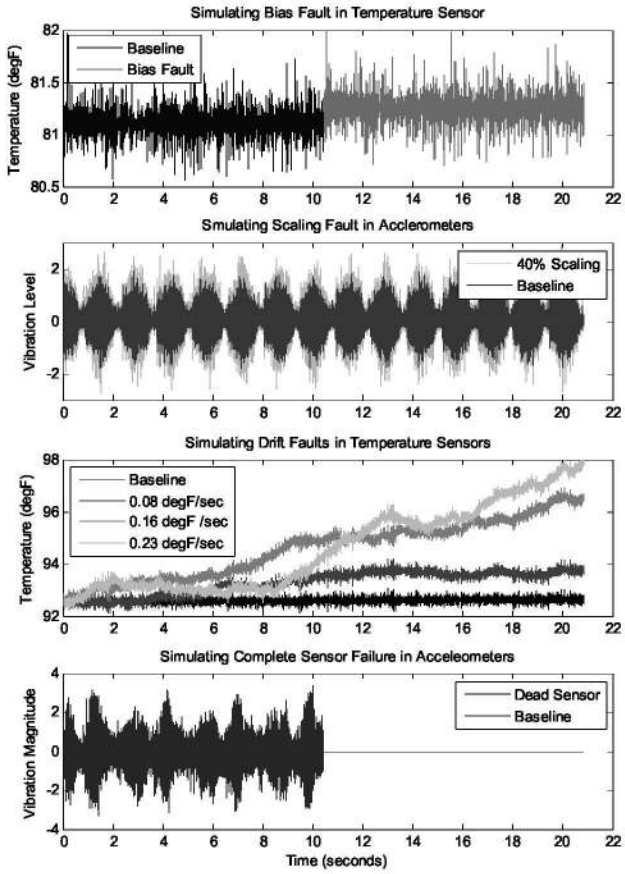

Fig. 10: Simulating various sensor faults in different sensor signals.

Drift: this fault was also injected into the nut temperature data. The fault was defined by specifying drift velocity (distance traveled in a certain period of time). The length of constant drift velocity segments was randomized (max 1000 data points) and Gaussian noise introduced into velocity value itself – so for each segment the velocity may be somewhat different from its neighbors. The signal-to-noise ratio for the later was set to 5.

Scaling: the signal is amplified by the scaling factor, also with Gaussian noise injected (SNR of 5).

Loss of Signal: sensor data from the point of failure replaced by all zeros.

VII. CLASSIFIER DIAGNOSTICS SYSTEM

Given the complexity of the experimental data and the variety of failure modes (actuator and sensor failures), a

diagnostic system based on Artificial Neural Networks (ANN) was designed. A comprehensive analysis of data was carried out to extract a set of uncorrelated features that would not only detect various fault modes but also disambiguate between sensor and system faults. Keeping this requirement of being able to disambiguate between system and sensor faults, the confusion matrix was further partitioned into sections that helped interpret results accordingly. This section explains the implementation details and enumerates various key aspect of the classifier diagnostic system.

A. Feature Extraction

Feature extraction is one of the most important steps in building a successful (accurate and reliable) diagnostic system. For a successful practical implementation it is desirable that features are not only be computationally inexpensive but also explainable in physical terms. Furthermore, they should be characterized by a) large between-class and small within-class variance, b) should be fairly insensitive to external variables like noise, and c) should be uncorrelated with other features. Keeping these issues in mind we selected a set of seven features that were expected to detect and distinguish between a healthy system, two actuator fault modes, and four different sensor faults (see Table 4).

TABLE 4. FAULT VS. FEATURE MATRIX SHOWING RELEVANCE OF INDIVIDUAL FEATURES IN DISAMBIGUATING BETWEEN VARIOUS FAULTS

Faults	Features					
	TD_{Nut}	TD_{Motor}	SD_x	SD_y	SD_Z	DI
Return Channel Ball Jam	X	X	X	X	X	
Spall			X	X	X	
Nut thermocouple Drift	X					X
Nut thermocouple Bias	X					
Z Accel. Scaling					X	
X Accel Complete Failure			X			

In addition, since there were several different experimental conditions that considerably affect the sensor measurements, two additional features were designed that characterize the experimental conditions. Features were calculated every half second on a one second long sliding window. Thus for each 90 second long segment, under various conditions, 180 feature points were available. These features are briefly described in Table 5.

TABLE 5 : VARIOUS FEATURES AS INPUTS TO THE CLASSIFIER FOR TRAINING AND TESTING EXPERIMENTS.

Feature	Sensors	Definition	Fault Modes	Rationale
Temperature Deviation (TD)	Nut thermocouple, Motor thermocouple	Absolute deviation from nominal temperature range	Spall, jam, sensor bias	Nut temperature rises due to increased friction from spalled nut. Motor temperature rises due to increased current levels to counter increased resistance Temperatures also change due to bias
Drift Indicator (DI)	Nut thermocouple, Motor thermocouple	A binary feature that assumes the value *one*, if a finite rate of change of temperature is detected within the sampling window, and *zero* otherwise	Sensor drift	Monitoring over some period of time can help identify sensor drift and distinguish it from bias, which is not expected to change continuously in shorter time-intervals
Signal Standard Deviation (SD)	Accelerometers: X, Y, Z on motor housing and one on the Nut	Standard deviation of the signal within one sampling window	Jam, dead sensor	Jam reflects in increased vibrations of the accelerometers mounted on the motor. Dead sensor results in zero output
Load Profile Indicator	Position sensor	Characterizes the smoothness of load profiles ranging between smooth sinusoids to rough triangular profiles	All	Nature of load the profile significantly changes the vibration signature of the system. This difference should be distinguished from failure signatures
Force Indicator	Position sensor	Assesses the force on actuator. For opposing force motion the force remains constant, proportional to peak loads. For spring motion force varies with the position and is a fraction of the peak loads	All	Given combinations of two different load conditions and two load application methods, differences in corresponding sensor signatures should be distinguished from fault signatures

B. Diagnostic Classifier

A multi-category classifier was implemented using a three layer Artificial Neural Network (ANN). The first layer consisted of nine nodes, with *tansigmoid* transfer functions, one for each feature in the input feature vector. The hidden layer had five nodes with *logsigmoid* transfer function and the output layer had seven nodes with *logsigmoid* transfer functions one for each of the seven classification categories. All input features were continuous real-valued and were standardized to have zero mean and unit variance [33]. Binary targets were assigned such that of the seven output bits only the correct category bit was 1 and the rest were 0. Initial weights for the network were chosen based on standardized

input ranges to ensure uniform learning [33]. Networks were trained using the resilient back-propagation (RPROP) algorithm [34].

C. Evaluation Procedure

Data was divided into two sets for training and testing purposes based on the experiment load levels. The network was trained on low load conditions (~900lbs) and was tested for high load (~1800lbs) conditions. In order to obtain a meaningful statistic, 30 ANNs were trained and tested for each experiment and the results averaged. Training was carried out for 200 epochs. Results were further aggregated in the form of a confusion matrix as shown below to observe the False Positive rate (FP), False Negative rate (FN), Misclassification rate (MC), and Non-Identification rate (NI). As expected, it was observed that the detection and disambiguation performance varied with changing sensor fault magnitudes. Therefore, a sensitivity analysis was carried out to characterize the effect of sensor failure magnitudes. For each of the three sensor faults drift, bias, and scaling corresponding fault parameter was varied one by one over a wide range of values while keeping other fault parameters fixed at a predetermined level derived from typical ranges available from the literature. More specifically, these predetermined values are temperature bias fixed at an offset of 100% of peak-to-peak magnitude, temperature drift fixed at 0.02 °F/sec, and scaling fixed at 1.5 times. The ranges of variation for these parameters are shown in Table 6.

TABLE 6. RANGES OF SENSOR FAULT PARAMETER VARIATION FOR CLASSIFIER SENSITIVITY ANALYSIS.

Sensor Fault	Min Value	Max Value
Bias	0	500% of peak-to-peak magnitude offset
Drift	0.005 °F/sec	0.25 °F/sec
Scaling	0.1x	5x

VIII. RESULTS AND DISCUSSION

Results were aggregated in two ways. First, the performance was evaluated in terms of sensitivity of metrics (FP, FN, MC, and NI) from the classifier for individual sensor faults. Therefore, if parameters for a sensor fault f_i, were varied, the effect was recorded only on the performance of classifier in classifying the sensor fault f_i, even though all other (system and sensor) fault modes were also present. Second, an overall performance assessment was made and an aggregate number was recorded for total FP, FN, MC, and NI rates for all faults combined as the intensity of a single sensor fault f_i was varied. The metrics for individual sensor faults are defined as follows.

False Positive: Sensor fault f_i is reported when no fault present.

False Negative: No fault reported when a sensor fault f_i present.

Misclassification: A system fault reported when sensor fault f_i present or sensor fault f_i reported when a system fault is present.

Non Identification: A fault detected but not identified when sensor fault f_i present.

As shown in Fig. 11, the diagnostic classifier implemented in this study is slightly sensitive to small drifts. For small drifts it becomes difficult to disambiguate between drift fault and baseline data, and hence a higher false negative rate. As drift velocity increases, it is easier to correctly identify a drift fault. The overall detection and disambiguation performance is within 5% FP, within 4% FN, less than 2% MC, and NI generally less than 8% except for low drift velocities where it is as high as 16% in some cases.

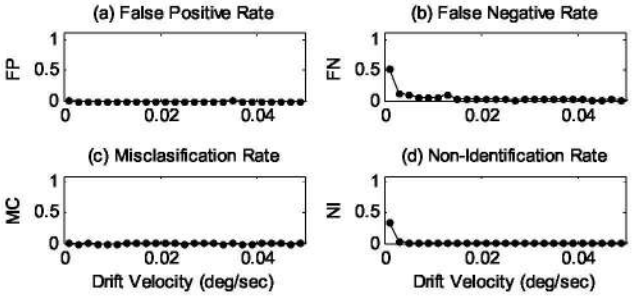

Fig. 11: Sensitivity of the classifier as drift velocity parameter changes.

Fig. 12 shows the classifier performance for bias sensor fault. Here the sensitivity of the classifier can be clearly seen. The reason for this sensitivity can, however, be attributed to two factors. First, for low bias there is a high false negative rate as it is difficult to distinguish from baseline data. Second, several fault modes, like ball jam and spall also result in increased operating temperatures, just like bias. However, since jam and spall are also reflected in other features that do not trigger in the presence of bias, a high non-identification rate is also observed. In terms of overall performance, once again less than 4% FP and FN are observed whereas NI goes as high as 18% for low values of bias. Misclassification rate is negligible.

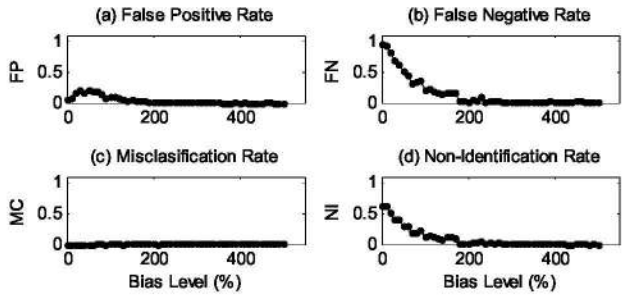

Fig. 12: Sensitivity of the classifier bias parameter changes.

Scaling fault detection performance deteriorates when scaling coefficient is close to one. As evident from Fig. 13, it's easier to detect both a down scaled signal or an up scaled signal but problems arise when fault signal is very identical to the healthy signal. For the scaling case, the overall NI rate was observed as high as up to 29% at scaling values close to one. FP rates remain low within 5%, FN within 4%, and MC less than 1% when combined for all fault scenarios.

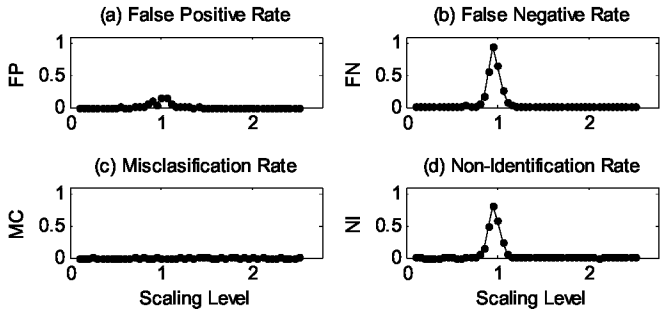

Fig. 13: Sensitivity of the classifier as scaling parameter changes.

Therefore, it can be concluded that in this study, the overall performance of the classifier, remains consistent with low FP, FN, and MC rates varying in the range of 0-7%, except for the NI rate which becomes high in more sensitive ranges for all three fault modes. Features are needed that are less sensitive to fault intensity parameters. The sensitivity analysis provides a useful insight into the fault classification problem where a classifier must be evaluated for all possible fault scenarios and designed to provide a more robust fault diagnosis.

IX. Plans for Future Work

There are a number of different avenues for future work. First, the set of sensors needs to be more exhaustively explored for sensors not covered in this article. While a first stab was taken at examining sensors of most interest within a narrow application domain, there is still a wide suite of unexplored sensors. In addition, other fault modes should be considered. While we have constrained this investigation to the faults occurring within the sensors themselves, a large number of faults associated with sensors are due to data acquisition (analog-to-digital converters, signal conditioning, etc.), electrical systems supporting sensor operation (power supplies), and other reasons. Moreover, some sensor fault types, such as intermittencies should be the subject of closer examination since they cause a large number of problems in real systems.

While in this work we have studied a classifier system that distinguished between sensor faults and system faults, it should be investigated how these classifiers (or reasoners) can be scaled to deal with large systems. This can be accomplished by a system-of-systems approach, by developing sensor fault tolerant schemes, or by modeling explicit or implicit function or analytical redundancies. Classifiers rely on features to allow optimal detection of sensor faults. While the features described herein focused mostly on time-domain features, other features (e.g., frequency-based feature) should be considered. In practice, sensor fault detection should go hand-in-hand with accommodation strategies. The understanding gained in the underlying mechanisms of sensor faults should be tapped into when considering new techniques for sensor accommodation. This should help in making system health management a more viable.

Another avenue for future work is the verification of the fault models developed. Experiments with seeded sensor faults on real systems should be conducted to confirm that the models behave correctly. To that end, plans are under way to carry out sensor fault experiments on a new actuator test stand at NASA Ames by manipulating sensors to induce certain types of faults and observe their signatures while the system operates under a variety of load conditions.Among other topics, it will aid in diagnostic and prognostic work for position measurement devices, such as LVDTs and resolvers/encoders, as one of the key feautures of the stand is an external, high-precision laser-triangulation position sensor

X.Conclusions

This paper has examined the physical underpinnings of sensor faults and has mapped them to five main categories. The ultimate goal has been to enable better systems health management by providing an insight into the behavior of sensor faults (as opposed to treating them as black box) which in turn might lead to improved fault accommodation strategies. In that spirit, a fault detector/classifier has been shown that successfully handles the set of faults under study for a wide range of fault parameters. A major contribution is the sensitivity of the classifier to variations of the fault parameters which identifies the regions in which sensor faults might pose a problem for the health reasoner. This approach might suggest a methodology of more generally developing and testing diagnostic systems on a wider range of possible sensor faults. A comprehensive analysis of sensor faults might ultimately lead to more robust system health management reasoners.

Acknowledgment

The authors would like to extend their gratitude to colleagues at the Prognostic Center of Excellence, NASA Ames Research Center for their extensive assistance with this research and preparation of the manuscript. They would also like to thank Paul Stoelting and Joel Rack at Moog Corporation for their efforts in producing and analyzing experimental data used in this project.

REFERENCES

[1] D. C. Zimmerman, and T. L. Lyde, "Sensor failure detection and isolation in flexible structires using the eigensystem realization algorithm," in 33rd Structural Dynamics and Materials Conference, Dallas, TX, 1992, pp. 2156-2166.

[2] S. S. Iyengar, and L. Prasad, "A general computational framework for distributed sensing and fault-tolerant sensor integration," *IEEE Transactions on Systems, Man, and Cybernetics,* vol. 25, no. 4, pp. 643-650, 1995.

[3] J. J. Gertler, "Survey of model-based failue detection and isolation in complex plants," *IEEE Control Systems Magazine*, no. December, pp. 11, 1988.

[4] J. G. Webster, *The measurement, instrumentation, and sensors handbook*, Boca Raton, FL: CRC Press, 1999.

[5] J. S. Wilson, *Sensor Technology Handbook*, Burlington, MA: Elsevier, 2005.

[6] "Omega technical reference," 2008-09-22; http://www.omega.com/techref/.

[7] J. G. Ternan, "Thermoelectric drift of thermocouples due to inhomogeneous changes in composition," *Journal of Applied Physics,* vol. 55, no. 1, pp. 199-209, 1983.

[8] T. Hamada, and Y. Suyama, "EMF drift and inhomogeneity of type K thermocouples," in SICE 2004 Annual Conference, Sapporo, Japan, 2004, pp. 989- 992.

[9] R. H. Bishop, *The mechatronics handbook*, Boca Raton, FL: CRC Press, 2002.

[10] L. Tong, D. Sun, and S. N. Atluri, "Sensing and actuating behaviours of piezoelectric layers with debonding in smart beams," *Smart Materials and Structures,* vol. 10, pp. 713-723, 2001.

[11] C. Li, and G. J. Weng, "Antiplane crack problem in functionally graded piezoelectric materials," *Journal of Applied Mechanics,* vol. 69, pp. 481-488, 2002.

[12] D. Wang, Y. Fotinich, and G. P. Carman, "Influence of temperature on the electromechanical and fatigue behavior of piezoelectric ceramics," *Journal of Applied Physics,* vol. 83, no. 10, pp. 5342-5350, 1998.

[13] "Strain gage knowledge base - technical notes," 2008-09-23; http://www.vishay.com/strain-gages/knowledge-base-list/.

[14] "MTS systems corporation," 2008-09-24; http://www.mtssensors.com/.

[15] A. E. Clark, J. B. Restorff, M. Wun-Fogle *et al.*, "Magnetostrictive Properties of Body-Centered Cubic Fe-Ga and Fe-Ga-Al Alloys," *IEEE Transactions on Magnetics,* vol. 36, no. 5, pp. 3238-3240, 2000.

[16] K. Goebel, and W. Yan, "Correcting sensor drift and intermittency faults with data fusion and automated learning," *IEEE Systems,* vol. 2, no. 2, pp. 189-197, 2008.

[17] S. J. Qin, and W. Li, "Detection and identification of faulty sensors with maximized sensitivity." pp. 613-617.

[18] P.-J. Lu, and T.-C. Hsu, "Application of autoassociative neural network on gas path sensor data validation," *Journal of Propulsion and power,* vol. 18, no. 4, pp. 879-888, 2002.

[19] D. C. Zimmerman, and T. L. Lyde, "Sensor failure detection and isolation in flexible structures using system realization redundancy," *AIAA Journal of Guidance, Control and Dynamics,* vol. 16, no. 3, pp. 490-497, 1993.

[20] C. D. Neppach, and V. A. Casdorph, "Sensor failure detection, identification and accommodation in a system without sensor redundancy," in 33rd Aerospace Sciences Meeting & Exhibit, Reno, NV, 1995.

[21] G. Rizzoni, and P. S. Min, "Detection of sensor failures in automotive engines," *IEEE Transactions on Vehicular Technology,* vol. 40, no. 2, pp. 487-500, 1991.

[22] S. Simani, C. Fantuzzi, and S. Beghelli, "Diagnosis techniques for sensor faults of inustrial processes," *IEEE Transactions on Control Systems Technology,* vol. 8, no. 5, pp. 848-855, 2000.

[23] J. J. Gertler, "Fault detection and isolation using parity equations," *Control Engineering Practice,* vol. 5, no. 5, pp. 653-661, 1997.

[24] S. Kim, Y. Kim, C. Park *et al.*, "Hybrid fault detection and isolation techniques for aircraft inertial measurement sensors," in AIAA Guidance, Navigation and Control Conference and Exhibit, Providence, RH, 2004.

[25] W. Chen, and M. Saif, "A sliding mode observer-based strategy for fault detection, isolation, and estimation in a class of Lipschitz nonlinear systems," *International Journal of Systems Science,* vol. 38, no. 12, pp. 943-955, 2007.

[26] C. P. Tan, and C. Edwards, "Sliding mode observers for detection and reconstruction of sensor faults," *Automatica,* vol. 38, pp. 1815-1821, 2002.

[27] E. Kiyak, Ö. Çetin, and A. Kahvecioglu, "Aircraft sensor fault detection based on unknown input observers," *Aircraft Engineering and Aerospace Technology,* vol. 80, no. 5, pp. 545-548, 2008.

[28] F. Gustafsson, "Stochastic fault diagnosability in parity spaces," in 15th IFAC World Congress, Barcelona, Spain, 2002.

[29] A. Hagenblad, F. Gustafsson, and I. Klein, "A comparison of two methods for stochastic fault detection and principal component analysis," in 13th IFAC Symposium on System Identification (SYSID), Rotterdam, NL, 2003, pp. 27-29.

[30] J. Litt, M. Kurtkaya, and A. Duyar, "Sensor fault detection and diagnosis simulation of a helicopter," in Conference of Military, Government, and Aerospace Simulation, San Diego, CA, 1994.

[31] P. Seda, E. Kadir, and B. Emine Dogru, "Intelligent sensor fault detection and identification for temperature control," in Proceedings of the 11th WSEAS International Conference on Computers, Agios Nikolaos, Greece, 2007.

[32] S.-J. Kim, and C.-W. Lee, "Diagnosis of sensor faults in active magnetic bearing system equipped with built-in force transducers," *IEEE Transactions on Mechatronics,* vol. 4, no. 3, pp. 180 - 186, 1999.

[33] R. O. Duda, P. E. Hart, and D. G. Stork, *Pattern Classification*, Second ed., p.^pp. 654, New York: John Wiley & Sons, Inc., 2000.

[34] M. Riedmiller, and H. Braun, "A Direct Adaptive Method for Faster Backpropagation Learning: The RPROP Algorithm," in IEEE International Conference on Neural Networks, San Fransisco, CA, 1993.

Edward Balaban is a researcher in the Diagnosis and System Health group at NASA Ames Research Center. His main areas of interest are diagnostics and prognostics of physical systems. He is currently the lead for actuator prognostics with the Diagnostics & Prognostics Group in the Intelligent Systems Division. During his years at Ames he participated in research and development of diagnostic and other autonomy elements for the X-34 experimental reusable launch vehicle, International Space Station, robotic astronaut assistants, autonomous planetary drills, and the future generation of autonomous micro-spacecraft. He received the Bachelor degree in Computer Science from The George Washington University in 1996 and the Master degree in Electrical Engineering from Cornell University in 1997.

Abhinav Saxena is a Staff Scientist with Research Institute for Advanced Computer Science at the Prognostics Center of Excellence, NASA Ames Research Center. His research focus lies in developing prognostic algorithms for engineering systems. He is a PhD in Electrical and Computer Engineering from Georgia Institute of Technology, Atlanta. He earned his B.Tech in 2001 from Indian Institute of Technology (IIT) Delhi, and Masters Degree in 2003 from Georgia Tech.

Prasun Bansal is an intern with Mission Critical Technologies at the Prognostics Center of Excellence, NASA Ames Research Center. His research focus lies in design & development of engineering systems and Multi Disciplinary Optimization. He earned Masters Degree in Aeronautics and Astronautics from Stanford University in 2008 and his B.Tech in Mechanical Engineering from Indian Institute of Technology (IIT) Delhi in 2006.

Kai Goebel received the degree of Diplom-Ingenieur from the Technische Universität München, Germany in 1990. He received the M.S. and Ph.D. from the University of California at Berkeley in 1993 and 1996, respectively. Dr. Goebel is a senior scientist at NASA Ames Research Center where he leads the Diagnostics & Prognostics groups in the Intelligent Systems division. In addition, he directs the Prognostics Center of Excellence and he is the Associate Principal Investigator for Prognostics for NASA's Integrated Vehicle Health Management Program. He worked at General Electric's Corporate Research Center in Niskayuna, NY from 1997 to 2006 as a senior research scientist. He has carried out applied research in the areas of artificial intelligence, soft computing, and information fusion. His research interest lies in advancing these techniques for real time monitoring, diagnostics, and prognostics. He holds ten patents and has published more than 100 papers in the area of systems health management.